THE JOURNAL OF PHYSICAL CHEMISTRY Letters

Letter

pubs.acs.org/JPCL

First-Principles Predictions of Vibrational Raman Optical Activity of Globular Proteins

Jiří Kessler,[†,‡] Josef Kapitán,[§] and Petr Bouř*[,†]

[†]Institute of Organic Chemistry and Biochemistry, Academy of Sciences, Flemingovo náměstí 2, 16610 Prague, Czech Republic

[‡]Department of Physical and Macromolecular Chemistry, Faculty of Science, Charles University, Hlavova 8, 12840 Prague, Czech Republic

[§]Department of Optics, Palacký University, 17. listopadu 12, 77146 Olomouc, Czech Republic

Supporting Information

ABSTRACT: Computational methods based on the Schrödinger equation have been traditionally confined to rather small molecules. Using an automatic computational methodology, however, we obtained a stunning agreement between experimental and theoretical vibrational spectra of large globular proteins containing thousands of atoms as well. Principle atomic properties are obtained from small molecular fragments and combined with a minimal accuracy loss. This "first-principles" interpretation of the data reveals a wealth of information, such as nature of localized molecular motions as well as collective vibrational modes describing folding of larger protein parts. A new insight is provided to the origin of the chiroptical effects, and the theory lends the used spectroscopic techniques, unpolarized Raman scattering and vibrational Raman optical activity, immense potential to structural studies of biological systems.

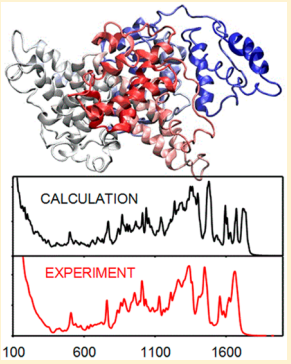

Recent advances in Raman spectroscopy revolutionized many domains including structural chemistry, biomedical research, and material science.[1,2] Raman optical activity (ROA) spectroscopy appears as one of these emerging techniques; it is sensitive to fine details in molecular structure including isotopic isomer effects[3] and has been applied to a plethora of systems including small molecules as well as whole viruses.[4,5] Because of their enhanced sensitivity to structural variations, such chiral spectroscopy techniques may be thought of as versatile alternatives to high-resolution approaches, such as X-ray diffraction. For solutions, they are often indispensable.

The polarization phenomena were linked to molecular structure already by Louis Pasteur;[6] however, only the recent advances in quantum chemistry made it possible to use the information provided by chiroptical experiments in full. Optical activity in the vibrational realm including ROA appears particularly attractive because it provides many well-resolved bands and intensities are tightly linked to the local molecular structure.[7] Note that this is often not the case in the electronic spectra.[8]

Yet after the discovery of molecular ROA[9] suitable computers and simulation and interpretation techniques were not immediately available. The subsequent development in the theoretical field included many steps, such as incorporation of the ROA intensity formulas in the quantum-chemical framework,[10] the origin-independent formulation,[11] and coupling of ROA with the density functional theory (DFT).[12]

Even within the DFT domain, however, it is difficult to simulate vibrational spectra of sizable molecules due to the unfavorable dependence of computational time on the number of atoms (N). This dependence, often referred to as "scaling", can be as sharp as N^5 for energy calculation by advanced DFT methods[13,14] and even less favorable for more accurate simulations or higher-order energy derivatives needed for ROA.[15] Clearly, alternative approaches need to be developed to efficiently combine spectroscopic and theoretical methods in structural biology.

In the present study, we use an automatized variant of the Cartesian coordinate transfer (CCT) technique to extend the quantum-chemical methodology for accurate simulations and understanding of ROA spectra of five different globular proteins. The CCT concept[16] is based on the locality of the molecular property tensors[17] that determine intensities and positions of spectral bands and the spring-like interatomic interactions involved in molecular vibrations. In the language of practical computations, we split the target molecule to chemically meaningful fragments, for which the relevant properties—tensors—can be obtained at high precision, for example, by DFT, and transfer them back to the target "atom by atom". Working in the Cartesian coordinates rather than in the previously used intrinsic coordinates is convenient if automatic computer routines are employed; the transfer then consists of fairly simple operations such as rotation and origin-dependence corrections. Although the method may introduce some error,[18,19] its precision is controllable and mostly

Received: July 14, 2015
Accepted: August 4, 2015
Published: August 4, 2015

DOI: 10.1021/acs.jpclett.5b01500
J. Phys. Chem. Lett. 2015, 6, 3314−3319

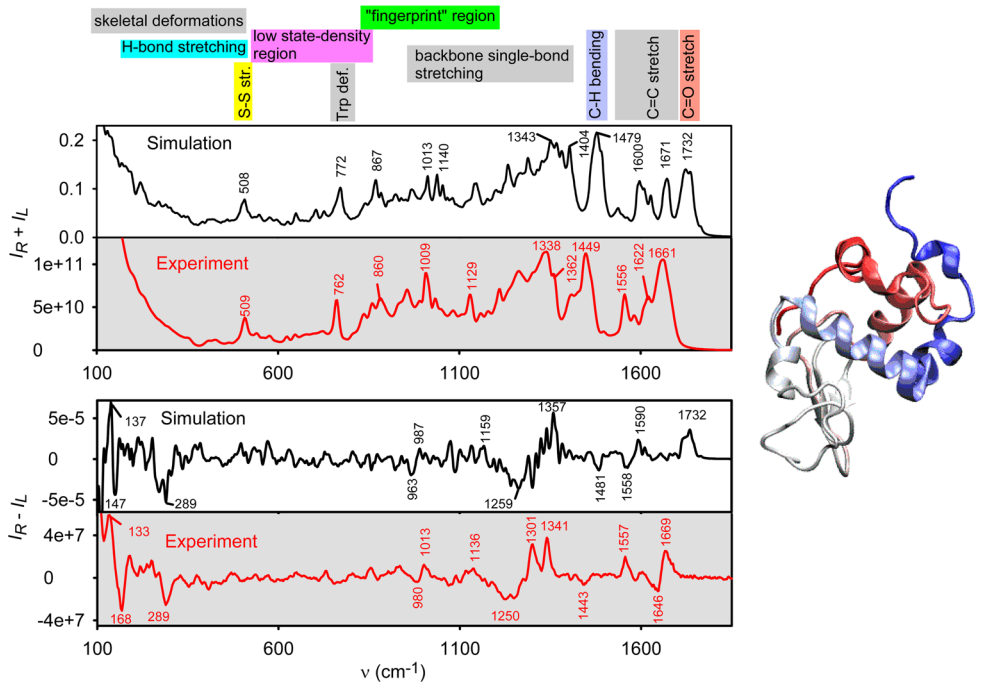

Figure 1. Comparison of calculated and experimental spectra. For bovine α-lactalbumin the Raman ($I_R + I_L$, top) and ROA ($I_R - I_L$, bottom) spectra obtained at the B3BPW91/6-31++G**/CPCM approximation level exhibit a surprisingly good correspondence with the experiment and allow for an accurate assignment of most vibrational bands. Selected vibrational classes are indicated at the top.

sufficient to explain experimental data.[20] For the globular proteins reported here, we achieved stunning accuracy in vibrational frequencies and spectral intensities so far achievable for comparable quantum chemical simulations in small molecules only.

Already early protein studies highlighted the sensitivity of ROA to backbone stereochemistry,[21] and the possibility to simulate and interpret the spectra from the first-principles significantly encouraged the development of the technique. Lately, a "brute force" DFT computation provided reasonable ROA spectra of the β domain of rat metallothionein.[22] Similarly, the CCT method helped us to understand the spectra and, more importantly, the solution structures of valinomycin[23,24] and insulin;[25] however, the much larger globular proteins explored in the present study could only be tackled after the fragmentation and transfer procedure was fully automated. To a certain extent, the transfer approach also makes it possible to explore the effect of conformational flexibility on the spectra, as many snapshots obtained from molecular dynamics can be averaged. The protein samples comprise bovine α-lactalbumin, concanavalin-A, hen egg-white lysozyme, human lysozyme, and human serum albumin. Concanavalin-A is an example of β-sheet-dominated protein; the others have a higher content of α-helix but exhibit finer structural differences. The human serum albumin is the largest molecule with the highest α-helical ratio.

Details of the protein structure and used computational methodology can be found in the Supporting Information. In the simplest case, X-ray protein geometry was divided into many overlapping four-amide residues, and these fragments were partially optimized using the vibrational normal mode coordinates[26] to preserve their conformation in the protein but relax principal vibrational motions. Then, vibrational spectroscopic parameters (force field, ROA tensors) were calculated at the B3PW91[27]/6-31++G**/CPCM[28,29] level using the Gaussian software[30] and transferred back to the protein. The Cartesian coordinate transfer procedure is described in detail elsewhere[16,20] and consists of the rotation of individual tensor components while taking into account their origin dependence. Note that absolute Raman intensities cannot be easily measured; the spectra are plotted in atomic and instrumental units for the simulation and experiment, respectively.

The reliability of the simulations is documented in Figure 1 for α-lactalbumin. The Raman intensity increases steeply and nearly monotonically toward the lowest-wavenumber region (300−100 cm^{-1}) because of the large signal and temperature excitations of the lowest-energy vibrational modes. The water background exhibiting similar trend has already been subtracted. Surprisingly, the ROA spectra (bottom part of Figure 1) provide quite distinct features also within this interval, and the experimental bands at 133, 168, and 289 cm^{-1} belong to the strongest ones in the entire ROA spectrum. The calculation reproduces them at 137, 147, and 289 cm^{-1} with the correct "+ − −" sign pattern. Visualization of the normal mode motion revealed that these bands are delocalized, mostly centered on the peptide main chain, but are difficult to assign to a particular chemical residue or local coordinate. Note that each visible band is composed of many individual transitions, as the density of vibrational states reaches ∼2.9 vibrational modes/cm^{-1} in this region.

Within the 300−900 cm^{-1} interval the density of vibrational states is relatively low, 2.1 modes/cm^{-1}. The simulation faithfully reproduces the most distinct spectral features such as the string S−S stretching (at 509/508 cm^{-1} in experiment/simulation) and tryptophan vibrations (762/772 and 860/867 cm^{-1}). The spectral intensities can thus be often related to local chemical coordinates. (Figure S5 and Tables S3 and S4 summarize these and other spectral features; see also refs 31−34 for vibrational assignment of protein ROA bands.) Typically, the strongest and relatively narrow Raman bands

DOI: 10.1021/acs.jpclett.5b01500
J. Phys. Chem. Lett. 2015, 6, 3314−3319

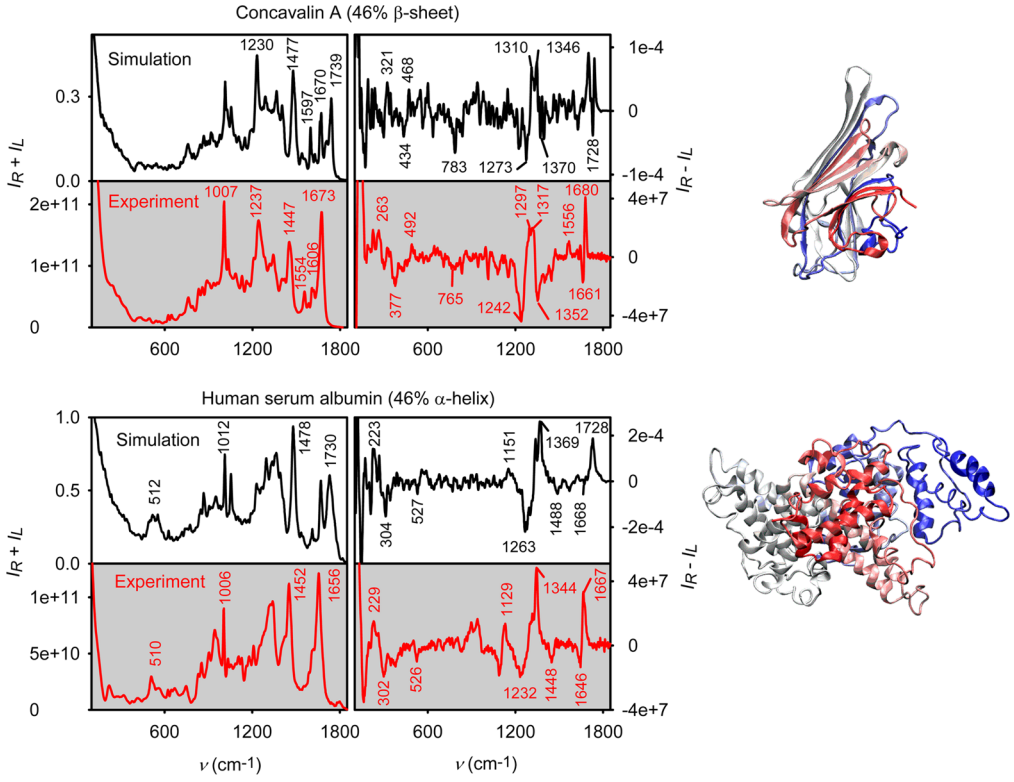

Figure 2. β sheet versus α-helical protein. Simulated and experimental Raman and ROA spectra of concavalin A and human serum albumin demonstrate sensitivity of both approaches in probing the peptide structure. For example, in concavalin, the 510 cm^{-1} Raman band of the disulfide bridges stabilizing the α-helical protein is missing, and the amide I frequency (1656 cm^{-1}) is very low due to the typical β-sheet interactions and band splitting. Even more differences may be found in the ROA spectra, as discussed in the main text.

originate in aromatic Trp, Phe, and Tyr amino acid residues; they exhibit a strong ROA signal as well. In ROA, however, the side chains' signals largely average out, and the resultant spectral shape is mainly due to the peptide main-chain contributions. In particular, in this wavenumber region the ROA intensities are rather weak, yet most of the experimental bands can be reproduced and assigned, as apparent from the expanded spectra (Figure S6). Within the 330−1130 cm^{-1} interval, for example, we counted about 23 Raman and ROA computed bands that probably match the experimental ones.

The 900−1400 cm^{-1} interval is a true "fingerprint" region with many overlapping vibrational bands and 3.3 vibrational modes/cm^{-1}; however, the overall character and the most distinct spectral features are reproduced as well, such as the Trp/Phe aromatic Raman signal around 1009 cm^{-1} and the Trp band at 1129 cm^{-1} (calculated at 1013 and 1140 cm^{-1}, respectively). This region comprises several distinct ROA bands, such as the negative signal at 980 cm^{-1} (largely peptide main chain deformation with a participation of C−C stretching reproduced at 963 cm^{-1}), the positive Trp band (exp./calc. 1013/987 cm^{-1}), and the broad negative lobe at 1250/1259 cm^{-1} of skeletal and amide vibrations. For vibrational spectroscopy of proteins, the so-called extended amide III spectral region (1280−1360 cm^{-1}) heavily involving $^{\alpha}$C−H bending is very important indeed.

The involvement of the peptide main chain groups in amide III vibrations and mode coupling makes ROA an excellent tool to monitor the secondary structure.[35] For example, α-helical structures exhibit two strong positive bands. The one at ∼1300 cm^{-1} was previously assigned to unhydrated canonical conformation and the 1340 cm^{-1} band attributed to a more open conformation stabilized by hydrogen bonding.[4] This assignment, based on empirical observation of α-helical peptides and proteins in polar and nonpolar solvents, did not explain all recorded data. In particular, poly(γ-benzyl-L-glutamate) in nonpolar $CHCl_3$ lacks the 1300 cm^{-1} "unhydrated" band. On the contrary, hydrated poly(L-lysine) or alanine-rich AK21 peptides do contain a strong 1300 cm^{-1} band.[4] Our computations suggest that these bands to a large extent originate in two $^{\alpha}$C−H bending modes in planes approximately parallel with and perpendicular to the $^{\alpha}$C−N bond (Figure S7). These are present in all conformers, and the intensity is varied through coupling to other vibrational modes.

Above 1400 cm^{-1} the vibrations become less dense again (2.3 modes/cm^{-1}) and can be assigned to local "chromophores" more easily, such as the C−H bending Raman signal at 1449/1479 cm^{-1} (exp./cal.), aromatic C═C stretching (1556/1600 cm^{-1} and 1622/1671 cm^{-1}), and, finally, the carbonyl "amide I" mode (largely C═O stretching, at 1661/1732 cm^{-1}). In the experimental ROA spectrum, the negative 1646 cm^{-1} peak is not well reproduced by the simulation, which in turn predicts a negative signal at 1558 cm^{-1}, with an experimental counterpart missing. The 1558 cm^{-1} band largely comes from induced optical activity of the tryptophan residues[36,37] and is thus very sensitive to conformational averaging. This and other minor inconsistencies can also be attributed to the anharmonicity and solvent effects that are only partially accounted for by the dielectric CPCM model and a limited precision of the DFT method causing improper mode ordering. In particular, the C═C aromatic stretching frequencies predicted by DFT are too high. The error of the CCT method, in particular the limited size of the fragments,[18,20] should also

DOI: 10.1021/acs.jpclett.5b01500
J. Phys. Chem. Lett. 2015, 6, 3314−3319

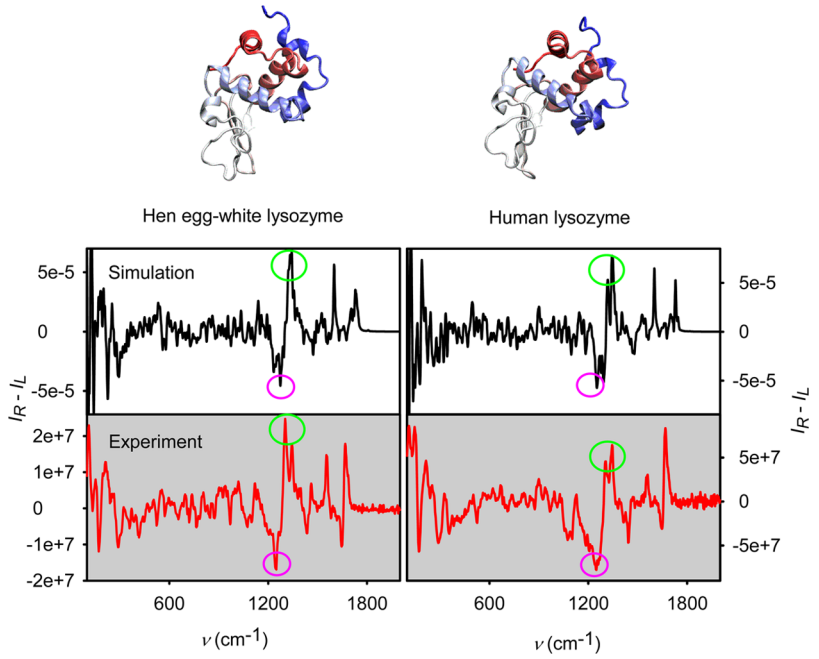

Figure 3. Reproducing fine structural differences. Calculated and experimental ROA spectra of hen and human lysozyme are compared. The two lysozymes have a very similar structure, and thus many differences are hidden in the experimental noise and computational error. However, some are detectable and can be reproduced. The encircled parts differ because of the different amounts of aromatic acids (Tyr, Phe) and their interaction with backbone and $^{\alpha}$C−H vibrations.

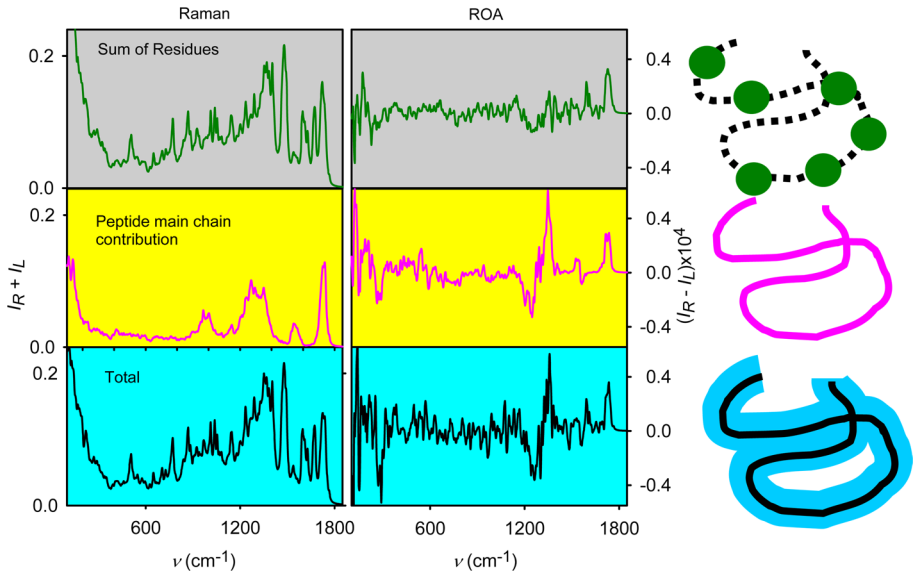

Figure 4. Contribution of protein parts to the Raman and ROA spectra. The Raman α-lactalbumin spectrum is approximately a sum of contribution of individual amino acids, whereas the ROA spectrum is dominated by the backbone signal sensitive to the secondary structure.

be considered, although it is supposed to be minor for irregular protein structures. Overall, however, the computation provides a solid ground for interpretation of the experimental data in this region. The ROA/Raman intensity ratio, often referred to as circular intensity difference (CID), is $\sim 3 \times 10^{-4}$, and it is reproduced by the simulations as well.

Raman and ROA spectra of concavalin A and human serum albumin are presented in Figure 2, as examples of predominantly β-sheet and α-helical structures, respectively. The Raman concavalin spectrum, when compared with α-lactalbumin, primarily reflects a different amino acid composition. The most obvious example is the absence of the disulfide bridges of cysteine and their Raman signal at 510 cm^{-1}. The ROA spectrum is more sensitive to the secondary structure, and the amino acid sequence is not so important. Unlike for α-lactalbumin, concavalin provides a predominantly positive signal in the low-wavenumber region (below 300 cm^{-1}), and a new negative band appears at 377 cm^{-1}. In the extended amide III region, the −/+/+ α-lactalbumin feature at 1250/1301/1341 cm^{-1} becomes a "−/+/+/−" pattern at 1242/1297/1317/1352 cm^{-1}, which is well reproduced by the calculation. The negative CH bending band changes to a weak −/+ couplet (1447/1474 cm^{-1}), and amide I couplet becomes stronger (−/+ lobes at 1661/1680 cm^{-1}).

DOI: 10.1021/acs.jpclett.5b01500
J. Phys. Chem. Lett. 2015, 6, 3314−3319

Human serum albumin with 9161 atoms is the largest structure in the set. Unlike for concavalin, its Raman spectrum (lower part in Figure 2) does not differ that much from α-lactalbumin (Figure 1); however, the larger α-helical content is reflected in ROA. The "α-helical" features slightly change; for example, the lowest positive ROA signal (133 cm^{-1} for α-lactalbumin) moves to 107 cm^{-1}, the negative 168 and 289 cm^{-1} bands are mostly conserved (at 162 and 302 cm^{-1}), and the same applies to the broad negative lobe around 1250 cm^{-1}. A more dramatic change occurs in the extended amide III region, where the positive ROA signal at 1344 cm^{-1} sharpens and the intensity increases. As for α-lactalbumin, there is a negative band of the CH bending at 1448 cm^{-1} and the predominantly positive amide I signal (maximum at 1667 cm^{-1}) is accompanied by a negative lobe (1646 cm^{-1}), and these features are reproduced to a large extent by the simulation. The α-helix/β-sheet differences are obviously more substantial, as apparent from the direct comparison of the human serum albumin and concavalin in Figure 2.

Although the hen and human lysozymes have very similar structures, their ROA spectra differ (Figure 3). In general, they are similar to those of α-lactalbumin, for example, in the "+/−/−" bands at ∼111/172/289 cm^{-1} and the broad "−/+" couplet centered around 1270 cm^{-1}. However, the hen lysozyme exhibits much sharper negative ROA band at 1250 cm^{-1} and a positive one at 1304 cm^{-1} than the human one, which is at least qualitatively reproduced by the simulations. Corresponding Raman spectra are plotted in Figure S8. A dynamic visualization of the vibrational normal modes reveals that the intensity changes can be to a large extent attributed to the different amino acid content. For example, the human lysozyme has twice as many Tyr residues as hen lysozyme. The aromatic vibrational modes are coupled to the main chain $^{\alpha}C-H$ bending, which makes the band at 1341 cm^{-1} (experiment) stronger. Several differences are also apparent for bands around 150 and 250 cm^{-1} and within 1350−1800 cm^{-1}.

To investigate in detail the link between various protein parts and the resultant spectral response, we constructed arbitrary spectra where Raman and ROA intensity tensors[17] of selected atoms were considered only. This is illustrated in Figure 4, where α-lactalbumin spectra are simulated (i) as a sum of individual amino acid residues, (ii) considering the peptide backbone atoms only, and (iii) involving all atoms. Note that the result has to be interpreted carefully as the total spectrum is not a simple sum of atomic contribution. Nevertheless, this computational exercise well documents the different character of the Raman and ROA signal: the Raman spectrum is approximately a sum of individual amino acid contributions, whereas ROA is dominated by the backbone signal. The importance of the backbone for the ROA intensity was confirmed by an alternate model, an all-alanine peptide of the same secondary structure as α-lactalbumin (Figure S9). These computational models clearly showed that the tight link to the backbone structure lends the ROA spectroscopy increased sensitivity to the conformation. At the same time, the backbone vibrations are heavily mixed with those of the side chains, and only the full-molecule simulation can explain the experimental data.

During the reviewing stage of this work an interesting question appeared: To what extent is it possible to actually reconstruct complete protein 3D solution structure "backward" from the ROA spectrum? This clearly remains a difficult task for a low-resolution technique. Nevertheless, the results above indicate that a systematic improvement in this respect is possible. Perhaps future experimental and theoretical advances can make the process more routine, resembling the combination of molecular modeling and experimental data usual in NMR protein studies already. One can, for example, think about combining MD/ab initio computations with empirical techniques recognizing specific spectral patterns.[38]

So far we can conclude that due to the automatic fragmentation procedure an unprecedented precision in frequencies and spectral intensities of five globular was achieved, so far achievable for small molecules only. The quantum-chemical accuracy is critical for correct interpretation of the experimental Raman and Raman optical activity protein spectra. In particular, it enabled us to relate fine spectral patterns to amino acid composition, local structural features, and peptide secondary structure. Differences in ROA intensities well reflected the β-sheet/α-helical differences, and the double-degenerate $^{\alpha}C-H$ vibration was assigned to the important conformational marker band around 1320 cm^{-1}. The theoretical apparatus thus makes the Raman and ROA spectroscopic methods versatile tools to study protein structure, for example, enhancing applications in biology and medical imaging.

■ ASSOCIATED CONTENT

Supporting Information

The Supporting Information is available free of charge on the ACS Publications website at DOI: 10.1021/acs.jpclett.5b01500.

Experimental and computational details documenting molecular properties and the spectral analysis. (PDF)

■ AUTHOR INFORMATION

Corresponding Author

*E-mail: bour@uochb.cas.cz.

Notes

The authors declare no competing financial interest.

■ ACKNOWLEDGMENTS

The present study was supported by the Grant Agency (P208/11/0105 and 15-09072S) and Ministry of Education (LM2010005 and CZ.1.05/3.2.00/08.0144) of the Czech Republic. We thank Dr. R. Pelc for useful comments on the manuscript.

■ REFERENCES

(1) Freudiger, C. W.; Min, W.; Saar, B. G.; Lu, S.; Holtom, G. R.; He, C.; Tsai, J. C.; Kang, J. X.; Xie, X. S. Label-Free Biomedical Imaging with High Sensitivity by Stimulated Raman Scattering Microscopy. *Science* **2008**, *322*, 1857−1861.

(2) Palonpon, A. F.; Ando, J.; Yamakoshi, H.; Dodo, K.; Sodeoka, S.; Kawata, S.; Fujita, K. Raman and SERS Microscopy for Molecular Imaging of Live Cells. *Nat. Protoc.* **2013**, *8*, 677−692.

(3) Haesler, J.; Schindelholz, I.; Riguet, E.; Bochet, C. G.; Hug, W. Absolute Configuration of Chirally Deuterated Neopentane. *Nature* **2007**, *446*, 526−529.

(4) McColl, I. H.; Blanch, E. W.; Hecht, L.; Barron, L. D. A Study of α-Helix Hydration in Polypeptides, Proteins, and Viruses Using Vibrational Raman Optical Activity. *J. Am. Chem. Soc.* **2004**, *126*, 8181−8188.

(5) Blanch, E. W.; McColl, I. H.; Hecht, L.; Nielsen, K.; Barron, L. D. Structural Characterization of Proteins and Viruses Using Raman Optical Activity. *Vib. Spectrosc.* **2004**, *35*, 87−92.

DOI: 10.1021/acs.jpclett.5b01500
J. Phys. Chem. Lett. 2015, 6, 3314−3319

(6) Pasteur, L. *Théses De Chimie Et De Physique*; Bachelier: Paris, 1847.
(7) Bouř, P.; Keiderling, T. A. Ab Initio Simulation of the Vibrational Circular Dichroism of Coupled Peptides. *J. Am. Chem. Soc.* **1993**, *115*, 9602−9607.
(8) Kaminský, J.; Kubelka, J.; Bouř, P. Theoretical Modeling of Peptide a-Helical Circular Dichroism in Aqueous Solution. *J. Phys. Chem. A.* **2011**, *115*, 1724−1742.
(9) Barron, L. D.; Buckingham, A. D. Rayleigh and Raman Scattering from Optically Active Molecules. *Mol. Phys.* **1971**, *20*, 1111−1119.
(10) Polavarapu, P. L.; Nafie, L. Vibrational Optical Activity: Comparison of Theoretical and Experimental Results for (+)-(3R)-Methylcyclohexanone. *J. Chem. Phys.* **1980**, *73*, 1567−1575.
(11) Helgaker, T.; Ruud, K.; Bak, K. L.; Jorgensen, P.; Olsen, J. Vibrational Raman Optical Activity Calculations Using London Atomic Orbitals. *Faraday Discuss.* **1994**, *99*, 165−180.
(12) Ruud, K.; Helgaker, T.; Bouř, P. Gauge-Origin Independent Density-Functional Theory Calculations of Vibrational Raman Optical Activity. *J. Phys. Chem. A* **2002**, *106*, 7448−7455.
(13) Schwabe, T.; Grimme, S. Double-Hybrid Density Functionals with Long-Range Dispersion Corrections: Higher Accuracy and Extended Applicability. *Phys. Chem. Chem. Phys.* **2007**, *9*, 3397−3406.
(14) Hudecová, J.; Profant, V.; Novotná, P.; Baumruk, V.; Urbanová, M.; Bouř, P. CF Stretching Region: Computational Modeling of Vibrational Optical Activity. *J. Chem. Theory Comput.* **2013**, *9*, 3096−3108.
(15) Ruud, K.; Thorvaldsen, J. Theoretical Approaches to the Calculation of Raman Optical Activity Spectra. *Chirality* **2009**, *21*, E54−E67.
(16) Bouř, P.; Sopková, J.; Bednárová, L.; Maloň, P.; Keiderling, T. A. Transfer of Molecular Property Tensors in Cartesian Coordinates: A New Algorithm for Simulation of Vibrational Spectra. *J. Comput. Chem.* **1997**, *18*, 646−659.
(17) Barron, L. D. *Molecular Light Scattering and Optical Activity*; Cambridge University Press: Cambridge, U.K., 2004.
(18) Bieler, N. S.; Haag, M. P.; Jacob, C. R.; Reiher, M. Analysis of the Cartesian Tensor Transfer Method for Calculating Vibrational Spectra of Polypeptides. *J. Chem. Theory Comput.* **2011**, *7*, 1867−1881.
(19) Yamamoto, S.; Bouř, P. On the Limited Precision of Transfer of Molecular Optical Activity Tensors. *Collect. Czech. Chem. Commun.* **2011**, *76*, 567−583.
(20) Yamamoto, S.; Li, X.; Ruud, K.; Bouř, P. Transferability of Various Molecular Property Tensors in Vibrational Spectroscopy. *J. Chem. Theory Comput.* **2012**, *8*, 977−985.
(21) Barron, L. D.; Hecht, L.; Blanch, E. W.; Bell, A. F. Solution Structure and Dynamics of Biomolecules from Raman Optical Activity. *Prog. Biophys. Mol. Biol.* **2000**, *73*, 1−49.
(22) Luber, S.; Reiher, M. Theoretical Raman Optical Activity Study of the B Domain of Rat Metallothionein. *J. Phys. Chem. B* **2010**, *114*, 1057−1063.
(23) Yamamoto, S.; Straka, M.; Watarai, H.; Bouř, P. Formation and Structure of the Potassium Complex of Valinomycin in Solution Studied by Raman Optical Activity Spectroscopy. *Phys. Chem. Chem. Phys.* **2010**, *12*, 11021−11032.
(24) Yamamoto, S.; Watarai, H.; Bouř, P. Monitoring the Backbone Conformation of Valinomycin by Raman Optical Activity. *ChemPhysChem* **2011**, *12*, 1509−1518.
(25) Yamamoto, S.; Kaminský, J.; Bouř, P. Structure and Vibrational Motion of Insulin from Raman Optical Activity Spectra. *Anal. Chem.* **2012**, *84*, 2440−2451.
(26) Bouř, P.; Keiderling, T. A. Partial Optimization of Molecular Geometry in Normal Coordinates and Use as a Tool for Simulation of Vibrational Spectra. *J. Chem. Phys.* **2002**, *117*, 4126−4132.
(27) Perdew, J. P.; Burke, K.; Wang, Y. Generalized Gradient Approximation for the Exchange-Correlation Hole of a Many-Electron System. *Phys. Rev. B: Condens. Matter Mater. Phys.* **1996**, *54*, 16533−16539.
(28) Klamt, A.; Jonas, V.; Burger, T.; Lohrenz, J. C. W. Refinement and Parametrization of COSMO-RS. *J. Phys. Chem. A* **1998**, *102*, 5074−5085.
(29) Mennucci, B.; Cappelli, C.; Cammi, R.; Tomasi, J. Modeling Solvent Effects on Chiroptical Properties. *Chirality* **2011**, *23*, 717−729.
(30) Frisch, M. J.; Trucks, G. W.; Schlegel, H. B.; Scuseria, G. E.; Robb, M. A.; Cheeseman, J. R.; Scalmani, G.; Barone, V.; Mennucci, B.; Petersson, G. A.; et al. *Gaussian 09*; Revision D01 ed.; Gaussian, Inc.: Wallingford, CT, 2009.
(31) Jacob, C. R.; Luber, S.; Reiher, M. Understanding the Signatures of Secondary-Structure Elements in Proteins with Raman Optical Activity Spectroscopy. *Chem. - Eur. J.* **2009**, *15*, 13491−13508.
(32) Jacob, C. R.; Luber, S.; Reiher, M. Analysis of Secondary Structure Effects on the IR and Raman Spectra of Polypeptides in Terms of Localized Vibrations. *J. Phys. Chem. B* **2009**, *113*, 6558−6573.
(33) Weymuth, T.; Jacob, C. R.; Reiher, M. Identifying Protein β-Turns with Vibrational Raman Optical Activity. *ChemPhysChem* **2011**, *12*, 1165−1175.
(34) Weymuth, T.; Reiher, M. Characteristic Raman Optical Activity Signatures of Protein β-Sheets. *J. Phys. Chem. B* **2013**, *117*, 11943−11953.
(35) Weymuth, T.; Jacob, C. R.; Reiher, M. A Local-Mode Model for Understanding the Dependence of the Extended Amide III Vibrations on Protein Secondary Structure. *J. Phys. Chem. B* **2010**, *114*, 10649−10660.
(36) Jacob, C. R.; Luber, S.; Reiher, M. Calculated Raman Optical Activity Signatures of Tryptophan Side Chains. *ChemPhysChem* **2008**, *9*, 2177−2180.
(37) Hudecová, J.; Horníček, J.; Buděšínský, M.; Šebestík, J.; Šafařík, M.; Zhang, G.; Keiderling, T. A.; Bouř, P. Three Types of Induced Tryptophan Optical Activity Compared in Model Dipeptides: Theory and Experiment. *ChemPhysChem* **2012**, *13*, 2748−2760.
(38) Zhu, F.; Tranter, G. E.; Isaacs, N. W.; Hecht, L.; Barron, L. D. Delineation of Protein Structure Classes from Multivariate Analysis of Protein Raman Optical Activity Data. *J. Mol. Biol.* **2006**, *363*, 19−26.

DOI: 10.1021/acs.jpclett.5b01500
J. Phys. Chem. Lett. 2015, 6, 3314−3319